JOURNAL OF NANO- AND ELECTRONIC PHYSICS
Vol. **10** No 3, 03004(6pp) (2018)

ЖУРНАЛ НАНО- ТА ЕЛЕКТРОННОЇ ФІЗИКИ
Том **10** № 3, 03004(6cc) (2018)

Numerical Simulation of SnS-Based Solar Cells

M.M. Ivashchenko[1,*], A.S. Opanasyuk[2,†], I.P. Buryk[1], D.V. Kuzmin[1]

[1] *Konotop Institute, Sumy State University, 24, Myru Ave., 41615 Konotop, Ukraine*
[2] *Sumy State University, 2, Rimsky-Korsakov Str., 40007 Sumy, Ukraine*

(Received 09 April 2018; published online 25 June 2018)

In this paper it was carried out the numerical simulation of the main working parameters (light current-voltage curves, quantum yield spectral distributions) of SnS-based (SnS/SnS_2/ITO, SnS/ZnS/ITO) solar cells (SCs) using the SCAPS-3102 simulation package. Using the basis input simulation parameters such as wide band gap E_g, layers thicknesses d, electron affinities χ, etc. there were estimated the next SCs characteristics: open-circuit voltages U_{OC}, short-circuit current densities J_{SC}, fill-factors FF and their efficiencies η. These data allows us to estimate the optimal constructive parameters of simulated SCs.

Keywords: Solar cell, Simulation, Fill factor, Efficiency, SCAPS.

DOI: 10.21272/jnep.10(3).03004 PACS numbers: 85.60.Bt, 78.20.Bh, 73.61.Ga

1. INTRODUCTION

Nowadays, the widening usage of photoelectric converters (solar cells – SCs) of photon irradiation energy is one of the ways of solution the global energy crisis [1]. For example, SCs based on CdTe semiconductor, such as based on CdTe/CdS hetero-junction, due to their acceptable energy conversion efficiency (more than 20 %) and to the optimal band gap value {E_g = 1.5 eV} are the most widely used thin-film photo-converters [2]. Unfortunately, CdTe/CdS-based SCs because of the cadmium presence are toxic and non-valuable for green-energy applications. On the last decade it was revealed the alternative for usage as absorber layer in high-efficiency SCs CIGS (Cu(In,Ga)S(Se)$_2$) ternary compounds [3]. But they consist of the scarity materials, such as indium (In) and gallium (Ga). So, these facts have motivated to search the alternative non-toxic and earth-abundant materials [4].

Tin mono-sulfide (p-SnS) and bi-sulfide (n-SnS_2) IV-VI group semiconductor compounds pay a higher attention of researchers due to their physical properties, such as: their band gap (BG) values which are closed to BGs of CdTe/CdS system (E_g = 1.34 eV – for SnS; E_g = 2.3 eV – for SnS_2 compounds) and may be used as an absorption (SnS) and window (SnS_2) layers in SCs [4 – 5]. Besides, these materials due to the relationship between sufficiency and their prices, have a great potential in solar energy conversion usage [2].

Another promising material in optoelectronics application is zinc sulphide (ZnS). Because of its BG value (E_g = 3.60-3.70 eV) this compound may be used as a window layer in tandem solar converters [2, 6]. In addition, it should be noted that all of these compounds (SnS, SnS_2, ZnS) do not contain a heavy and toxic metal – cadmium (Cd) for example, which is very important in ecological aspects [7 – 9].

In recent time the efficiency of SnS-based SCs is equal to 2-3 % [3, 10]. So, the further possibility of their energy conversion efficiency may be improved by optimizing its deposition condition, such as: thicknesses of SCs layers – absorption, window, buffer or conduction layers; operation temperature, etc. [11]. These processing conditions formed the aim of this work – the numerical simulation of the SCs working parameters (open-circuit voltage U_{OC}, short-circuit current density J_{SC}, fill-factor FF, efficiency η) as a function of the layers characteristics and the exploitation temperature.

2. NUMERICAL SIMULATION PROCESSING

The light current-voltage characteristics (I-V curves) and dependencies "quantum efficiency – wavelength" (QE) were modeled by us using the simulation package SCAPS-3102 [3, 11-12]. The simulation process is based on Poisson's equation:

$$\frac{d^2}{dx^2}\psi(x) = \frac{e}{\varepsilon_0\varepsilon_r}(p(x) - n(x) + N_D - N_A + \rho_p - \rho_n) \quad (1)$$

where Ψ is electrostatic potential; e is an electron charge; ε_r is relative and ε_0 is vacuum dielectric permittivity; p and n are hole and electron concentrations; N_D (N_A) are charged impurities of donor (acceptor) types; ρ_p(ρ_n) are holes and electrons distributions [13].

The continuous equations for electrons and holes are presented below:

$$\frac{d}{dx}J_n(x) - e\frac{\partial n(x)}{\partial t} - e\frac{\partial \rho_n}{\partial t} = G(x) - R(x) \quad (2)$$

$$\frac{d}{dx}J_p(x) + e\frac{\partial p(x)}{\partial t} + e\frac{\partial \rho_n}{\partial t} = G(x) - R(x) \quad (3)$$

where J_n and J_p are electron and hole current densities; $G(x)$ and $R(x)$ are charge generation and recombination rates [13].

SCAPS simulation package allows us to calculate I-V curves and EQ dependencies respectively. Additionally, the recombination in deep levels and their filling is described by the Shockley-Read-Hall formalism. Recombination levels at the interfaces are calculated using the

* m_ivashchenko@ukr.net
† opanasyuk_sumdu@ukr.net

extension of the Shockley-Read-Hall formalism connected to the exchange of electrons between the junction states and energy bands (valence and conduction, respectively). In SCAPS package the interface states may be distributed by energy values. The metal–semiconductor (contact-layer) junction is processed by thermion emission of charge carriers (Bethe theory) [13].

Schematic structure of SCs design based on SnS/SnS_2(ZnS)/ITO structure is presented on Fig. 1. ITO (indium-tin-oxide) was selected by us as an upper conduction layer due to its *n*-type of conductivity and light-transparency nature [11].

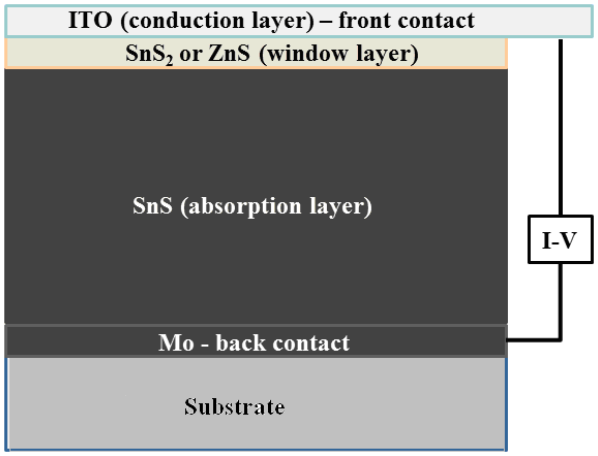

Fig. 1 – Schematic structure of simulated SCs

Before the start of simulation procedure it needs to select the input layers simulation parameters, such as: absorption, window and conduction layers thicknesses (*d*), BG values (E_g), their electron affinities (χ) and dielectric constants ($\varepsilon/\varepsilon_0$), electrons ($\mu_n$) and holes ($\mu_p$) mobility, their effective masses (m_n/m_0 and m_p/m_0, respectively), densities of states in conduction (N_C) and valence (N_V) bands, etc [11].

The main input simulation parameters are given on Table 1.

Table 1 – The input simulation parameters

Layer	SnS	SnS_2	ZnS	ITO
Parameters				
E_g, eV	1.34	2.24	3.68	3.68
X, eV	4.20	4.24	4.45	4.80
$\varepsilon/\varepsilon_0$, a.u.	16.00	6.19	8.30	8.90
N_C, cm^{-3}	$8.90\cdot10^{18}$	$5.10\cdot10^{17}$	$6.34\cdot10^{18}$	$5.20\cdot10^{18}$
N_V, cm^{-3}	$1.00\cdot10^{18}$	$2.24\cdot10^{18}$	$1.46\cdot10^{19}$	$1.00\cdot10^{18}$
μ_n, cm^2/s	100	50	30	10
μ_p, cm^2/s	25	20	7	10
m_n/m_0	-	0.21	0.40	0.30
m_p/m_0	0.50	-	-	-

The simulation process is carried out using the following starting modeling conditions: solar irradiation zone AM 1.5; Three of four (SnS thickness, SnS_2{ZnS} thickness, ITO thickness, operation temperature) simulation parameters were as usual fixed while the fourth of them was changed.

3. RESULTS AND DISCUSSION

The thickness of the basis (absorption) layer is an important working parameter of SCs due to its ability of the charge carrier absorbance and probable solar conversion efficiency improving [11].

On Fig. 2 and Table 2 are presented the simulation results of SnS/SnS_2/ITO and SnS/ZnS/ITO SCs with

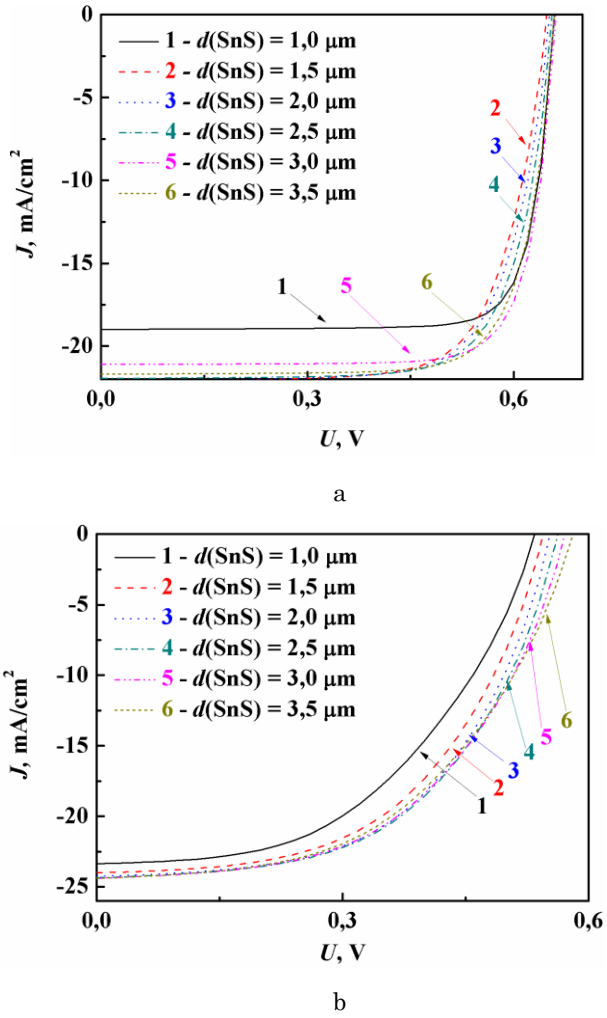

Fig. 2 – Light I-V curves of SCs with the structure SnS/SnS_2ITO (a) and SnS/ZnS/ITO (b) at different thicknesses of the SnS absorption layer

Table 2 – SCs working characteristics at different SnS absorption layer thicknesses

d, nm	U_{OC}, V	J_{SC}, mA/cm^2	*FF*, %	η, %
SnS/SnS_2/ITO				
1000	0.66	18.99	80.91	10.13
1500	0.65	22.17	71.80	10.32
2000	0.65	22.09	72.62	10.47
2500	0.66	21.94	74.16	10.68
3000	0.66	21.10	79.05	11.02
3500	0.66	21.68	76.48	10.93
SnS/ZnS/ITO				
1000	0.53	23.36	49.60	6.19
1500	0.54	24.00	53.78	7.03
2000	0.55	24.24	54.98	7.38
2500	0.56	24.34	54.36	7.44
3000	0.57	24.38	52.95	7.38
3500	0.58	24.39	51.15	7.25

changing the absorption layer thickness. As a starting condition, the thicknesses of two other layers were constant – $d_{SnS2(ZnS)}$ = 25 nm, d_{ITO} = 25 nm.

Analysis of *I-V* curves shown that in both cases of modeled solar cells it was observed that at increasing of the SnS layer thickness from 1.0 to 3.5 μm in both cases the open-circuit voltage U_{OC} is negligible oscillated (U_{OC} = 0.65-0.66 V in case of SnS/SnS2/ITO and U_{OC} = 0.53-0.58 V in case of SnS/ZnS/ITO); short-circuit current density in both cases is significantly increased – from 18.99 mA/cm² to 22.17 mA/cm² and some decreased to 21.68 mA/cm² in case of SnS/SnS2/ITO; in case of SnS/ZnS/ITO SC J_{SC} was permanently increased from 23.36 mA/cm² to 24.39 mA/cm², while the absorption layer's thickness was increased.

In both cases of simulated solar cells it was observed the complex changing of efficiency: in case of SnS/SnS2/ITO SC the solar cell efficiency at the increasing of SnS layer thickness from 1.0 μm to 3.0 μm is increased from 10.13 % to 11.02 %, after that while the SnS layer's thickness reached to 3.5 μm η is some decreased to 10.93 %. Similar view is observed in case of SnS/ZnS/ITO SC where efficiency value was increased from 6.19 % to 7.44 % and some decreased to 7.25 %. This effect may be caused by the total light irradiation absorption at the SnS layer thickness of: 3.0 μm in case of SnS/SnS2/ITO and 2.5 μm in case of SnS/ZnS/ITO. At these values of absorption layer thickness a number of generated electron-hole pairs reached to saturation. Further layer thickness increasing improves the increasing of the series-resistance [8]. So, as a result of the performed calculations, it is evaluated that obtained optimal values of 3.0 μm (SnS/SnS2/ITO) and 2.5 μm (SnS/ZnS/ITO) might be used in further calculations. The mismatch between d_{ZnS} values may be caused y the difference of the carrier generation regions and energy band values [14 – 15].

On Fig. 3 and Table 3 are presented the results of SCs simulation with different window layer thickness, which is an important working parameter because of its allowable of determination the amounts of irradiation entering the absorption layer [11].

As a result of calculations it was determined that in case of SnS/SnS2/ITO SC the value of U_{OC} at SnS_2 layer increasing from 25 to 200 nm was constant (0.66 V). Besides, in case of SnS/ZnS/ITO SC the U_{OC} value was negligible decreased from 0.56 V to 0.53 V. In both cases of calculated SCs at window layer increasing J_{SC} values were significantly decreased from 23.54 mA/cm² to 19.54 mA/cm² (SnS/SnS2/ITO) and from 24.34 mA/cm² to 20.45 mA/cm² (SnS/ZnS/ITO). The SCs efficiency in both cases is also some decreased while the window layer value is increased. It may be caused by the increasing of the photons absorbing in window layer while increasing of their thickness [11].

It should be noted that obtaining continuous SnS_2 or ZnS films with thickness lesser than 25 nm is very difficult, so, the simulation processing of window layers (and ITO conduction layer) with thickness d < 25 nm is not performed.

It was determined that optimal window layer thickness values are: in case of SnS/SnS2/ITO – 25 nm;

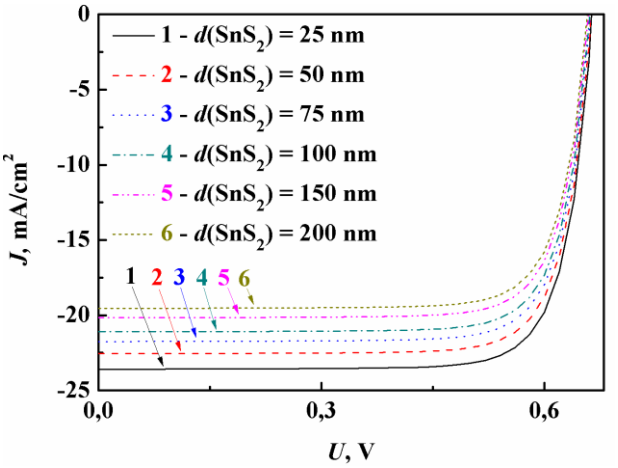

a

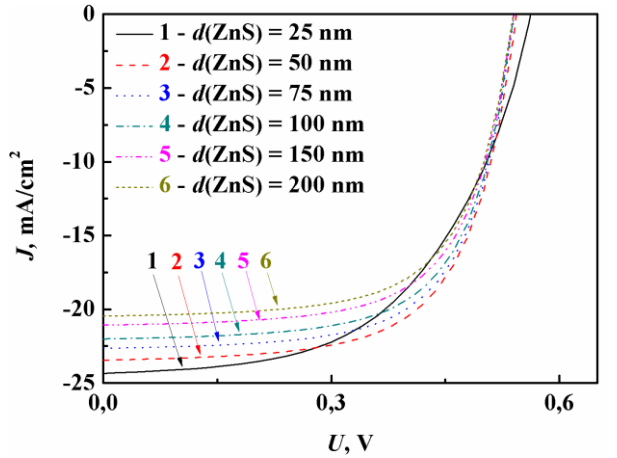

b

Fig. 3 – Light I-V curves of SCs with the structure SnS/SnS2ITO (a) and SnS/ZnS/ITO (b) at different thicknesses of the SnS_2 (ZnS) window layer

Table 3 – SCs working characteristics at different SnS_2 (ZnS) window layers thicknesses

d, nm	U_{OC}, V	J_{SC}, mA/cm²	FF, %	η, %
SnS/SnS2/ITO				
25	0.66	23.54	79.30	12.42
50	0.66	22.55	79.20	11.84
75	0.66	21.74	79.12	11.39
100	0.66	21.10	79.05	11.02
150	0.66	20.16	78.96	10.50
200	0.66	19.54	78.91	10.15
SnS/ZnS/ITO				
25	0.56	24.34	54.36	7.44
50	0.54	23.44	64.86	8.26
75	0.54	22.64	65.72	8.05
100	0.53	22.00	65.66	7.81
150	0.54	21.07	65.46	7.45
200	0.54	20.45	65.32	7.21

in case of SnS/ZnS/ITO – 25 nm, respectively. These data are used in further calculations.

On Fig. 4 and Table 4 are presented the results of SCs simulation with different thickness of ITO conduction layer (front contact).

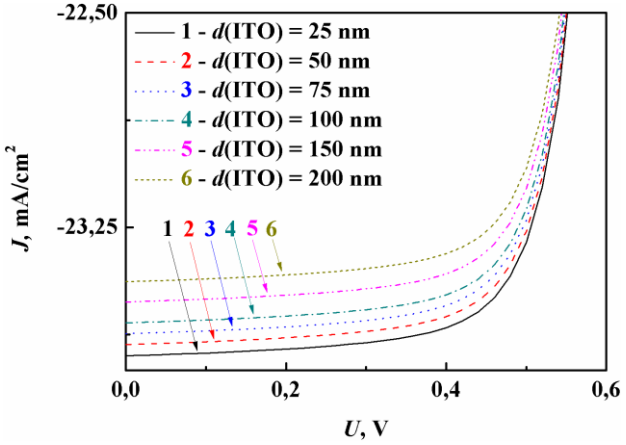

a

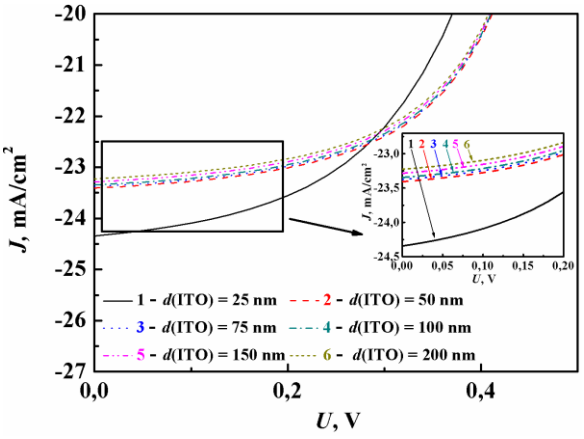

b

Fig. 4 – Light *I-V* curves of SCs with the structure SnS/SnS_2ITO (a) and SnS/ZnS/ITO (b) at different thicknesses of the ITO conduction layer

Table 4 – SCs working characteristics at different ITO conduction layer thicknesses

d, nm	U_{OC}, V	J_{SC}, mA/cm²	FF, %	η, %
SnS/SnS_2/ITO				
25	0.66	23.70	79.30	12.49
50	0.66	23.66	79.31	12.47
75	0.66	23.62	79.30	12.44
100	0.66	23.58	79.30	12.42
150	0.66	23.51	79.29	12.38
200	0.66	23.44	79.29	12.34
SnS/ZnS/ITO				
25	0.56	24.34	54.36	7.44
50	0.54	23.41	64.87	8.25
75	0.54	23.38	64.88	8.24
100	0.54	23.35	64.89	8.23
150	0.54	23.28	64.91	8.21
200	0.54	23.23	64.92	8.19

It was determined that in both cases the value of η while ITO layer thickness was increased from 25 nm to 200 nm is negligible changed – some decreased in case of SnS/SnS_2/ITO SCs; some increasing in case of SnS/ZnS/ITO SCs. In both cases $\Delta\eta \leq 0.5$ %. This fact allows us to use ITO conducting layer with minimal thickness – 25 nm because of the presence in this compound indium (In) rare element.

There were estimated the optimal ITO layer thickness conditions for simulated SCs: $d_{ITO} = 25$ nm for SnS/SnS_2/ITO and $d_{ITO} = 50$ nm for SnS/ZnS/ITO structures, respectively.

During their exploitation SCs can be warming up in the operation of solar irradiation. This fact would be significantly influenced on the SCs working parameters. So, we studied the influence of operation temperature on processing characteristics of SnS/SnS_2/ITO and SnS/ZnS/ITO SCs in the range of 290-340 K with optimized layers thicknesses values, determined by us earlier. The results of simulation are presented on Fig. 5 and Table 5.

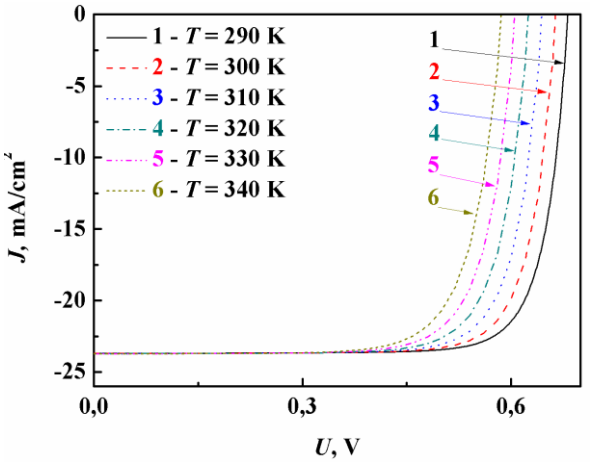

a

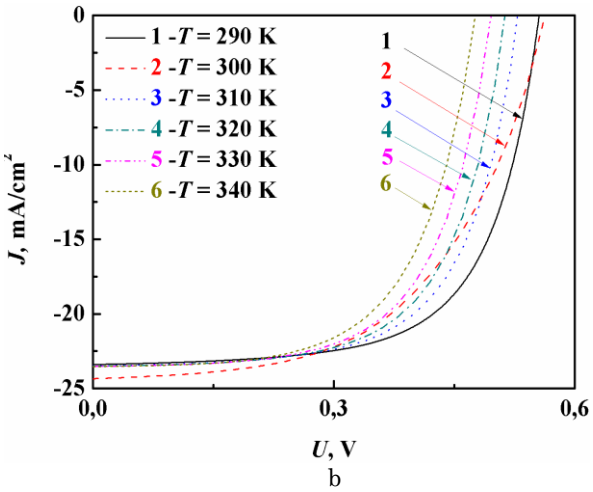

b

Fig. 5 – Light *I-V* curves of SCs with the structure SnS/SnS_2ITO (a) and SnS/ZnS/ITO (b) at different operating temperatures

In both cases of calculated structures the value of energy conversion efficiency η is significantly decreased at increasing of the operation temperature (from 13.00 % {290 K} to 10.45 % {340 K} for SnS/SnS_2/ITO structure; from 8.50 % {290 K} to 6.91 % {340 K} for SnS/ZnS/ITO structure, respectively). Calculated data are physically-correct because the increasing of operation temperature T leads to decreasing of layers BGs, so it performs the decreasing of the heterojunction contact potential difference.

Dependences of quantum efficiency of calculated

Table 5 – SCs working characteristics at different operation temperatures

T, K	U_{OC}, V	J_{SC}, mA/cm²	FF, %	η, %
SnS/SnS₂/ITO				
290	0.68	23.69	80.26	13.00
300	0.66	23.70	79.30	12.49
310	0.65	23.70	78.30	11.97
320	0.63	23.71	77.26	11.46
330	0.61	23.71	76.19	10.95
340	0.59	23.71	75.10	10.45
SnS/ZnS/ITO				
290	0.56	23.39	65.27	8.50
300	0.56	24.34	64.36	7.44
310	0.53	23.48	64.36	8.00
320	0.51	23.50	63.71	7.69
330	0.50	23.52	62.82	7.33
340	0.48	23.53	61.65	6.91

SCs with different physical and technological features of structure components design are presented on Fig. 6.

It should be noted that calculated SCs are photosensitive in wide range of the wavelengths.

On Fig. 7 are presented the generalized dependences of designed SCs – fill factor FF and efficiency η as a function of selected simulation conditions.

4. CONCLUSIONS

It was performed the numerical simulation of the SnS/SnS₂/ITO and SnS/ZnS/ITO solar There were obtained light I-V curves and spectral dependences of quantum efficiency. As a result of the simulation there were determined the optimal design parameters which provide their maximal efficiency. It was performed the

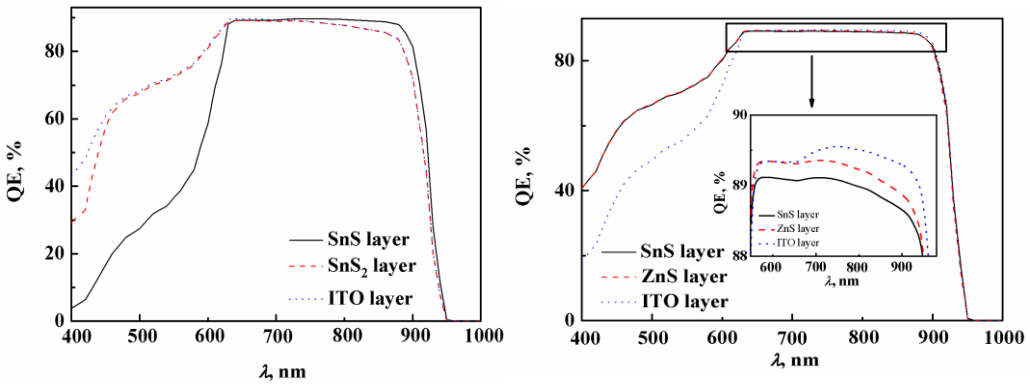

Fig. 6 – Dependences of the quantum efficiency of SCs with the structure SnS/SnS₂ITO (a) and SnS/ZnS/ITO (b) on the heterosystem layers thicknesses

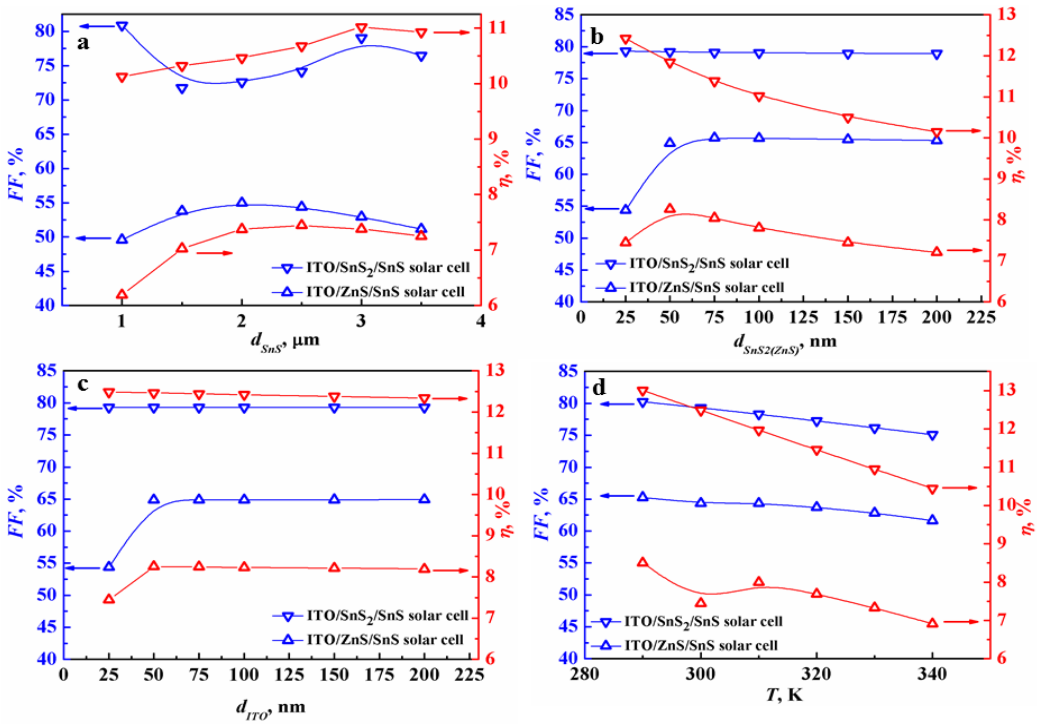

Fig. 7 – Variations of fill-factor FF and SCs efficiency η as a function of: SnS absorption layer thickness d_{SnS} (a); SnS_2 (ZnS) window layer thickness $d_{SnS2(ZnS)}$ (b); ITO conduction layer thickness d_{ITO} (c) and operation temperature T (d)

numerical simulation of the SnS/SnS$_2$/ITO and SnS/ZnS/ITO solar There were obtained light *I-V* curves and spectral dependences of quantum efficiency.

As a result of the simulation there were determined the optimal design parameters which provide their maximal efficiency. They are: for SnS/SnS$_2$/ITO structure – d_{SnS} = 3.0 μm, d_{SnS2} = 25 nm, d_{ITO} = 25 nm, T = 290 K; for SnS/ZnS/ITO structure – d_{SnS} = 2.5 μm, d_{ZnS} = 50 nm, d_{ITO} = 50 nm, T = 290 K, respectively. Optimal working characteristics of simulated solar cells are: for SnS/SnS$_2$/ITO structure – U_{OC} = 0.68 V, J_{SC} = 23.69 mA/cm^2, FF = 80.26 %, η = 13.00 %; for SnS/ZnS/ITO structure – U_{OC} = 0.56 V, J_{SC} = 23.29 mA/cm^2, FF = 65.27 %, η = 8.50 %, respectively.

AKNOWLEDGEMENTS

This work was supported by the Ministry of Education and Science of Ukraine (Grant # 0116U006813).

Числове моделювання сонячних елементів на основі SnS

М.М. Іващенко[1], А.С. Опанасюк[2], І.П. Бурик[1], Д.В. Кузьмін[1]

[1] *Конотопський інститут, Сумський державний університет, пр. Миру, 24, 41615 Конотоп, Україна*
[2] *Сумський державний університет, вул. Римського-Корсакова, 2, 40007 Суми, Україна*

В даній роботі проведене числове моделювання основних експлуатаційних характеристик (світлові вольт-амперні характеристики, спектральні розподіли квантової ефективності) сонячних елементів (СЕ), виконаних на базі шару SnS (SnS/SnS$_2$/ITO, SnS/ZnS/ITO) з використанням програмного пакету SCAPS-3102. Обравши такі базові характеристики для моделювання, як ширина забороненої зони E_g, товщини шарів d, спорідненості електронів χ, тощо, були отримані наступні експлуатаційні характеристики СЕ: напруга холостого ходу U_{OC}, густина струму короткого замикання J_{SC}, фактор заповнення FF та коефіцієнт корисної дії фотоперетворення η. Отримані значення дозволили визначити оптимальні конструктивні параметри змодельованих сонячних елементів.

Ключові слова: Сонячний елемент, Моделювання, Фактор заповнення, К.К.Д., SCAPS.

Численное моделирование солнечных элементов на базе SnS

М.Н. Иващенко[1], А.С. Опанасюк[2], И.П. Бурык[1], Д.В. Кузьмин[1]

[1] *Конотопский институт, Сумский государственный университет, пр. Мира, 24, 41615 Конотоп, Украина*
[2] *Сумский государственный университет, ул. Римского-Корсакова, 2, 40007 Сумы, Украина*

В данной работе было проведено численное моделирование основных эксплуатационных характеристик (световые вольт-амперные характеристики, спектральное распределения квантовой эффективности) солнечных элементов (СЭ), исполненных на основе слоя SnS (SnS/SnS$_2$/ITO, SnS/ZnS/ITO) с использованием программного пакета SCAPS-3102. Избрав такие характеристики для моделирования, как ширина запрещенной зоны E_g, толщины слоев d, электронное сродство χ, и т.д., были получены следующие эксплуатационные характеристики СЭ: напряжение холостого хода U_{OC}, плотность тока короткого замыкания J_{SC}, фактор заполнения FF и коэффициент полезного действия фотопреобразования η. Полученные значения позволили определить оптимальные конструктивные параметры смоделированных солнечных элементов.

Ключевые слова: Солнечный элемент, Моделирование, Фактор заполнения, К.П.Д., SCAPS.

REFERENCES

1. A. Yago, T. Kibushi, Y. Akaki, S. Nakamura, *Jpn. J. Appl. Phys.* **57** No 2, 02CE08 (2018).
2. A.S. Opanasyuk, D.I. Kurbatov, M.M. Ivashchenko, I.Yu. Protsenko, *J. Nano- Electron. Phys.* **4** No 1, 01024 (2012).
3. H. Movla, E. Abdi, D. Salami, *Optik* **124**, 5871 (2013).
4. P. Sinsermsuksakul, K. Hartman, S. Kim, J. Heo, *Appl. Phys. Lett.* **102**, 053901 (2013).
5. A. Voznyi, V. Kosyak, P. Onufrijevs, L. Grase, *J. Alloy Compd.* **688**, 130 (2016).
6. B. Siahmardan, V. Soleimanian, M. Varnamkhasti, *Mat. Sci. Semicon. Proc.* **71**, 76 (2017).
7. A. Basak, A. Hati, A. Mondal, U.P. Singh, *Thin Solid Films* **645**, 97 (2018).
8. S.S. Hedge, A.G. Kunjomana, P. Murahali, B.K. Prasad, *Surf. Interf.* **10**, 78 (2018).
9. N.K. Samani, Z.D. Tafti, H.A. Bioki, M.B. Zarandi, *Optik* **131**, 231 (2017).
10. D. Lim, H. Suh, M. Surawanshi, G.Y. Song, *Adv. Energy Mater.* **8**, 1702605 (2018).
11. A.S. Opanasyuk, M.M. Ivashchenko, I.P. Buryk, V.A. Moroz, *J. Nano- Electron. Phys.* **7** No 2, 02037 (2015).
12. A. Kumar, A.D. Thakur., Mater. Sci., arXiv:1510.05092v1.
13. H. Movla, *Optik* **125**, 67 (2014).
14. Y. Xiang, Y. Yang, F. Guo, X. Sun, *Appl. Surf. Sci.* **435**, 759 (2018).
15. V. Robles, J.F. Trigo, C. Guillen, J. Herrero, *Thin Solid Films* **582**, 249 (2015).